Rheological and Thermal Properties of Narrow Distribution Poly(ethyl acrylate)s

L. Andreozzi,*,† V. Castelvetro,‡ M. Faetti,† M. Giordano,† and F. Zulli†

Department of Physics "E. Fermi", University of Pisa, largo B. Pontecorvo 3, 56127 Pisa, Italy; CNR, INFM, polyLab, largo B. Pontecorvo 3, 56127 Pisa, Italy; and Department of Chemistry and Industrial Chemistry, University of Pisa, via Risorgimento 35, 56124 Pisa, Italy

Received October 10, 2005; Revised Manuscript Received December 31, 2005

ABSTRACT: In the present work, we characterize the rheological behavior of 10 nearly monodisperse poly(ethyl acrylate) samples, whose molar mass ranges from 1200 to 150 000 g/mol. The poly(ethyl acrylate)s were obtained by means of a controlled/living radical polymerization technique. The time−temperature superposition principle works, and the T dependence of the horizontal shift factor $a_{Tr}(T)$ is fairly well described by the Williams−Landel−Ferry law. Furthermore, the zero-shear viscosity dependence on the temperature, for all the investigated samples, has resulted to be well described by means of Vogel−Fulcher laws. The mass dependence of thermal parameters such as the Vogel temperature T_0 and the pseudo-activation energy T_b has been worked out and compared to the mass dependence of the glass transition temperature T_g. This leads us to propose here a coherent way to describe their behavior and estimate several microscopic parameters in terms of free volume. Moreover, the molar mass dependence of material parameters has been investigated. The zero-shear viscosity η at different temperatures has been evaluated, and the critical mass value has been found to be $M_c = 26\,000$ g/mol. The ratio between the critical M_c and the entanglement mass M_e has been found to be about 2.2 from the evaluation of the plateau modulus G_N^0. A mass dependence analysis of the steady-state compliance J_e^0 has also been carried out from which the second critical mass M_c' is inferred.

1. Introduction

The viscoelastic and mechanical properties of polymeric materials are strongly affected by structure, conformation, and molar mass of the chain. In particular, the polymer molar mass influences directly the topological properties of polymer melts, which regulate the onset and the dynamics of the entangled regime, usually modeled by using the reptation concept.[1] A strong indication of chain entanglement coupling, that is the presence of temporary networks in the polymer, is the steep increase of zero-shear viscosity with polymeric mass M around a value of critical mass M_c[1,2] according to the relationships

$$\eta \propto M \qquad M < M_c \tag{1a}$$

$$\eta \propto M^{3.4} \qquad M > M_c \tag{1b}$$

Another indication of chain entanglement is the modulus plateau G_N^0 observed in high molar mass nearly monodisperse samples from which it is evaluated the mass M_e between the entanglements.[2] The ratio M_c/M_e is usually found to be in the range 2.0−2.4.

In the past decades, several physical quantities such as terminal relaxation time τ_0 and steady-state compliance J_e^0 have also been correlated to molar mass and polydispersity of polymers.[3,4] The mass dependence of the steady-state compliance of polymers shows the effects of entanglements, when the molar mass is decreased, in correspondence of a second critical mass M_c', as a change from a plateau regime to the linear dependence predicted by the Rouse model.[1]

The precise occurrence of entanglement is the topic of a recent thread in the literature (see for example ref 5). As a matter of fact, when the entanglement is present in chain melts, several macroscopic quantities are constant, while at low masses they decrease with decreasing molar mass. The mass dependence of the fitting parameters T_b and T_0, from the Vogel−Fulcher law[6−8] (see eq 3) of the viscosity η, and c_1 and c_2, from Williams−Landel−Ferry law[2] (see eq 4) of the shift factor $a(T)$, have been analyzed in terms of the molar mass as well as the glass transition temperature T_g, this latter fundamental in the thermal characterization of polymeric materials. All these quantities follow a molar mass behavior, which discriminates the entanglement dynamics and could be interpreted in terms of the free volume theory.[2]

Polyacrylates have been for a long time of difficult synthesis: acrylates have long been known to undergo controlled polymerization by anionic mechanism, but there is poor control on the molar mass and molar mass distribution when primary acrylates with short alkyl chain, such as methyl and ethyl acrylates, are employed. The poly(ethyl acrylate) (PEA) samples used in this work were obtained[9] following a recent developed atom transfer polymerization technique.[10]

This work aims to characterize the melt rheology and thermal properties of poly(ethyl acrylate)s with narrow molecular weight distribution. In particular, the mass dependence of T_b, T_0, and T_g has been analyzed according to the free volume concept, and a coherent way of describing their molar mass behavior is proposed here. Such a study led to the determination of the asymptotic values, in the presence of entanglement, of these physical quantities, which can be expressed in terms of several microscopic quantities.

Moreover, the comparison of the fitting parameters, drawn from the functional relationship here proposed to describe the mass dependence of the above parameters, allowed us to evaluate the ratio between the free volume pertinent to the

* To whom correspondence should be addressed: e-mail laura.andreozzi@df.unipi.it.
† Department of Physics and polyLab.
‡ Department of Chemistry and polyLab.

10.1021/ma052190+ CCC: $33.50
Published on Web 02/04/2006

Table 1. Chemical and Physical Characterization of Poly(ethyl acrylate) Samples[a]

sample	CuBr/EBP (mol ratio)	conv (%)	t_p[13] (h)	M_n (g/mol)	M_w (g/mol)	M_w/M_n	M_z (g/mol)	M_z/M_w	T_g (K)
PEA01R	1.0	98	4	7500	8250	1.10	9250	1.09	248
PEA02R	1.0	98	4	11650	13100	1.13	15200	1.12	252
PEA04R	1.0	98	4	18650	20200	1.08	22200	1.07	250
PEA05R[14]	1.0	50	4	24900	26600	1.07	29300	1.07	253
PEA06R	1.0	71	64	58200	66500	1.15	90000	1.16	253
PEA15R[15]	0.1	85	21	980	1200	1.22	1500	1.20	231
PEA16R[15]	0.2	82	21	2750	3000	1.09	3300	1.08	243
PEA17R[15]	0.5	81	21	7300	7800	1.07	8700	1.06	247
PEA18R	0.5	60	5	8800	9600	1.09	10500	1.09	250
PEA20R[16]	4.5	64	96	120000	150000	1.25	220000	1.25	253

[a] M_n, M_w, and M_z are the first three molar mass averages.[12]

polymeric chain and chain tail. This is particularly interesting because PEA polymers were synthesized with terminating units as much as possible similar to the ethyl acrylates monomeric units, allowing the comparison of the ratio obtained in this study with theoretical findings of the literature.[11]

A study of the material parameter plateau modulus G_N^0 and of the mass dependence of zero-shear viscosity η and steady-state compliance J_e^0 has also been carried out. In these cases, the discrimination between the Rouse and the entanglement regimes is apparent, and a correlation between macroscopic fitting parameters and microscopic quantities is carried out. Thus, we have been able to determine the product $\zeta_0 b^2$ between the monomeric friction coefficient ζ_0 and the segment length b as well as the ratio between the polymeric characteristic masses M_e, M_c, and M_c'.

2. Materials and Experiment

PEA samples were prepared by atom transfer radical polymerization (ATRP), using 2-bromoethyl propionate (2-EBP) as initiator, which becomes indistinguishable from the ethyl acrylate (EA) repeat unit once inserted in the macromolecular chain. The complex of CuBr with the polydentate aminoaliphatic ligand (PMDETA) was employed as the catalyst for the reaction (Table 1). When compared with polypyridine ligands, polyamines lower the redox potential of the Cu(I)/Cu(II) couple, thus allowing a smooth polymerization to take place at low temperatures ($T < 373$ K) and thereby reducing the possibility of side reactions.

Ethyl acrylate (12 g, 0.12 mol), anisole (13 mL, 4.6 mol/L, in the case of polymerization in solution), CuBr, and *N*,*N*,*N*′,*N*″,*N*″-pentamethyldiethylenetriamine (PMDETA 1/1 weight ratio with respect to CuBr) were introduced in a Schlenk tube and stirred a few minutes to allow complex formation. The initiator 2-EBP was then added to the stirred green homogeneous mixture, followed by degassing with three freeze−pump−thaw cycles.

The polymerization was then carried out at 363 K for about 4 h (bulk) or 24−60 h (solution). The copper catalyst was removed by column chromatography over alumina using $CHCl_3$ as eluent. Because of the high solubility or swell ability of poly(ethyl acrylate) in most organic solvents, quantitative removal of the unreacted monomer was achieved only after prolonged (about 1 week) drying at 343 K under high vacuum (1 mmHg). Mass spectrometry analysis of the resulting polymers showed the presence of <100 ppb residual monomer, according to an EA area calibration curve.

Number-average M_n and weight-average M_w molar masses, and polydispersity, defined as the ratio M_w/M_n, were determined by size exclusion chromatography (SEC) performed at room temperature on 0.050 mL samples (4 g/L polymer solutions in chloroform) at 1 mL/min flux, using a Waters 515 HPLC pump, a PL-Gel Mixed-C column, and a Waters 2410 RI detector (see Table 1). Six monodisperse polystyrene standards (1460, 300, 83, 19, 4, and 0.8 kg/mol) were used for column calibration. The molar mass data are referred to a calibration curve, which was a third-order polynomial fit from polystyrene standards. Gas chromatograph and mass spectrometer (GC-MS) analyses were carried out on a Varian 3800 GC equipped with a Varian VA-5 capillary column (30 m, 0.25 mm, 0.25 μm, 5% phenylmethylpolysiloxane) coupled with a Varian Saturn 2000 Ionic Trap MS. In this work, the density ρ of PEA samples is taken as 1.12 g/cm^3.[17]

Differential calorimetry measurements were performed with a DSC7 Perkin-Elmer calorimeter on the samples in order to obtain glass transition temperature (T_g) values according to the onset definition. This apparatus was calibrated with indium and zinc standards. The thermograms were recorded on heating at 10 K/min after a quench at 40 K/min.

Physical data resulting from PEA samples characterization are reported in Table 1 together with the experimental details of the synthesis of PEAs with different molar masses.

Viscoelastic properties were measured with a Haake RheoStress RS150H stress-controlled rheometer. The deformation is detected with a digital encoder processing 1 million impulses per revolution, pushing the resolution of the measurements at very low strains. The cone−plate geometry (35 mm diameter, cone angle 4°) has been utilized for measurements on the lightest sample PEA15R, while a parallel plate system (diameter 20 mm) has been utilized for all other samples. To account for thermal dilatation of the system, as the temperature was varied, the gap in the parallel plate geometry was varied in the range between 900 and 1100 μm for all the polymer samples except PEA20R, for which measurements were carried on with a gap of 1400−1600 μm. The gaps were chosen significantly larger than chain lengths to ensure gap-independent measurements.

The thermostat system of RS150H is equipped with a thermal bath of circulating fluid with programmable temperature. While the upper plate of the RS150H is crossed by the thermostat fluid only, the lower plate consists of a Peltier system which drives and maintains at the set value the temperature at the sample, while exchanging heat with the thermal bath. The rheometer plate system is embedded in a glass cylindrical tube. A flux of ultrapure nitrogen gas is injected into the cell to avoid aqueous condense on performing measurements at temperatures lower than the ambient one.

Preliminary tests on linear viscoelastic regime of the materials were conducted to carry out all measurements in this regime. Isothermal frequency sweeps were measured from 10^{-2} to 24.4 Hz. Zero-shear viscosity η was evaluated in independent ways from creep and flow experiments at different temperatures and from the complex modulus in oscillatory measurements.

3. Results

In Figure 1, the temperature dependence of the viscosity, as obtained from the creep and flow measurements in a large temperature interval, is shown for the different PEA samples. In Figure 1, zero-shear viscosities are also reported (open symbols) as calculated from the loss modulus G'' in the terminal zone according to the equation

$$\lim_{\omega \to 0} \frac{G''(\omega)}{\omega} \tag{2}$$

In Figure 2 some $G''(\omega)$ data recorded at different temperatures

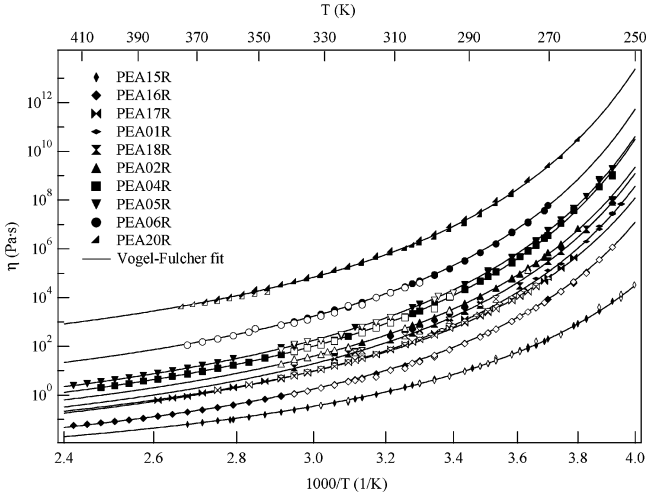

Figure 1. PEA's zero-shear viscosity as a function of 1000/T from steady-state (filled symbols) and dynamic (open symbols) measurements.

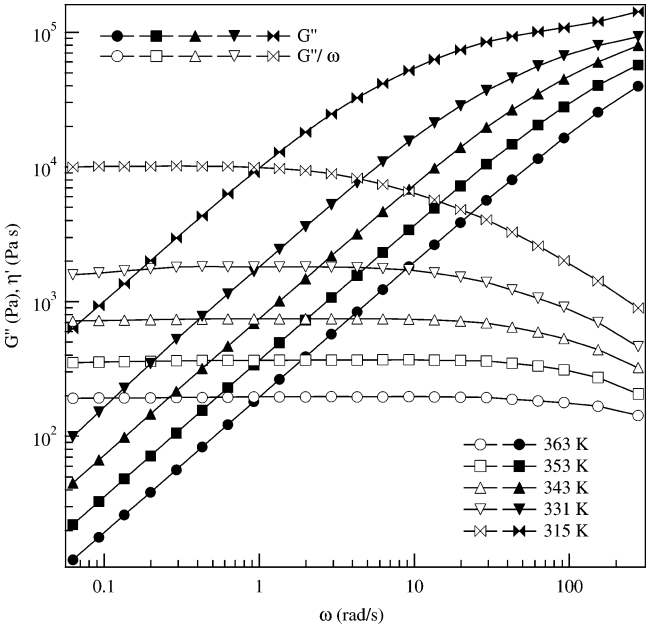

Figure 2. Examples, at different temperatures, of the curves used to evaluate the zero-shear viscosity of PEA06R from the loss modulus G'' according to eq 2. $\eta' = G''/\omega$ is the real part of the complex viscosity η^*.

are shown for the sample PEA06R. The zero-shear viscosity η of each sample, within the temperature range 260−400 K, is well reproduced (Figure 1) by Vogel−Fulcher (VF) laws:[6−8]

$$\eta(T) = \eta_\infty \exp\left(\frac{T_b}{T - T_0}\right) \tag{3}$$

The values of the prefactors η_∞, the pseudo-activation energies (expressed in kelvin) T_b, and the Vogel temperatures T_0 are reported in Table 2.

On the other hand, within the temperature range from T_g + 7 K up to T_g + 160 K, the time−temperature superposition (TTS) principle was found to be applicable. As an example, in Figure 3 the master curves of PEA05R, PEA06R, and PEA20R storage moduli G' as well as tan $\delta = G''/G'$ are shown at the reference temperature T_r = 270 K.

The horizontal and vertical shift factors $a_{Tr}(T)$ and $b_{Tr}(T)$ at the reference temperature T_r, as well as the master curves, are

Table 2. Vogel−Fulcher Fit Parameters of Zero-Shear Viscosity of PEAs, Which Are Listed in Order of Increasing Molar Mass M_w

sample	η_∞ (Pa s)	T_b (K)	T_0 (K)
PEA15R	$(1.6 \pm 0.1) \times 10^{-4}$	1070 ± 40	194 ± 3
PEA16R	$(1.4 \pm 0.1) \times 10^{-4}$	1260 ± 40	200 ± 3
PEA17R	$(5.1 \pm 0.4) \times 10^{-4}$	1310 ± 60	200 ± 4
PEA01R	$(3.3 \pm 0.3) \times 10^{-4}$	1360 ± 50	201 ± 6
PEA18R	$(4.9 \pm 0.4) \times 10^{-4}$	1400 ± 30	201 ± 3
PEA02R	$(8.6 \pm 0.8) \times 10^{-4}$	1430 ± 30	200 ± 4
PEA04R	$(1.3 \pm 0.1) \times 10^{-3}$	1480 ± 40	202 ± 3
PEA05R	$(2.1 \pm 0.2) \times 10^{-3}$	1500 ± 40	201 ± 4
PEA06R	$(2.2 \pm 0.2) \times 10^{-2}$	1480 ± 40	202 ± 7
PEA20R	$(8.0 \pm 0.8) \times 10^{-1}$	1490 ± 40	202 ± 3

Table 3. WLF Parameters of $a_{Tr}(T)$ at the Reference Temperature T_r = 270 K; PEAs Are Listed in Order of Increasing Molar Mass M_w

sample	c_1[19]	c_2 (K)[19]	c_1c_2 (K)	$T_0 = T_r - c_2$ (K)
PEA15R	6.2	76	470	194
PEA16R	7.3	71	520	199
PEA17R	7.9	70	555	200
PEA01R	8.0	69	555	201
PEA18R	8.6	69	590	201
PEA02R	8.9	69	610	201
PEA04R	9.0	68	610	202
PEA05R	9.1	68	620	202
PEA06R	9.1	68	620	202
PEA20R	9.2	68	625	202

obtained in this work by mathematical shifting[18] of experimental isotherm frequency sweeps of the complex modulus $G^*(\omega)$. The horizontal shift factors $a_{Tr}(T)$ are well described by the semiempirical Williams−Landel−Ferry (WLF) law:[2]

$$\log a_{Tr}(T) = \frac{-c_1(T - T_r)}{T - T_r + c_2} \tag{4}$$

c_1 and c_2 are the WLF parameters, and T_r is the reference temperature. The values of the WLF T_r-dependent parameters c_1 and c_2 as well as the invariants c_1c_2 and $T_0 = T_r - c_2$ for the PEA samples are found in Table 3.

From the master curves of PEAs, the plateau modulus G_N^0 can be experimentally determined by adopting different definitions.[20−22] We followed the criterion of the minimum of tan $\delta = G''/G'$. At the frequency where tan δ is minimum,[1,23,24] one sets

$$G_N^0 = G'(\omega : \tan\delta \text{ min}) \tag{5}$$

Accordingly, the plateau modulus G_N^0 can be evaluated for those PEA samples only with M_w greater than M_c, being tan δ monotonically decreasing with increasing frequency for masses less than M_c.

The storage moduli G' master curves, as well as tan δ, of PEA05R, PEA06R, and PEA20R at T_r = 270 K are shown in Figure 3 as a function of the frequency. From all these three samples, within the experimental errors, the value $G_N^0 = (2.1 \pm 0.1) \times 10^5$ Pa is found, resulting to be mass-independent, as expected for amorphous linear homopolymers. The same criterion has been used to determine G_N^0 at 291 and 305 K; the values $G_N^0 = (2.2 \pm 0.1) \times 10^5$ Pa and $G_N^0 = (2.4 \pm 0.1) \times 10^5$ Pa have been found. According to the TTS principle,[2] the plateau modulus varies with temperature following the T dependence of the vertical shift parameter $b_{Tr}(T)$.

From the master curves it is also possible to evaluate another important parameter in the characterization of the rheological properties of poly(ethyl acrylate)s: the steady-state shear

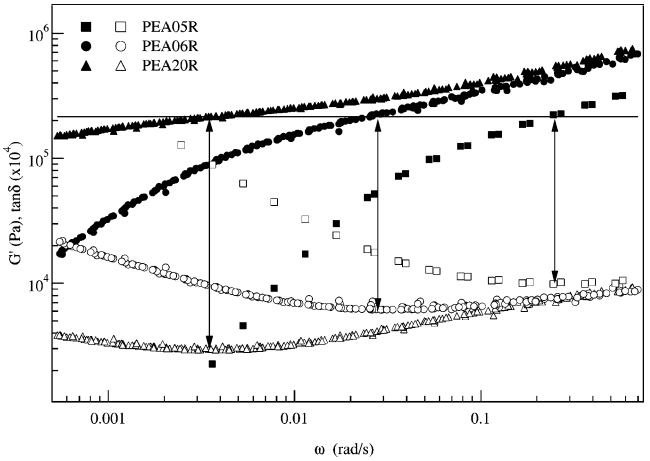

Figure 3. Master curves of the storage modulus G' (filled marks) of PEA05R, PEA06R, and PEA20R reduced at the reference temperature $T_r = 270$ K. The value of the plateau modulus G_N^0, from the minimum $\tan\delta = G''/G'$ (empty marks) criterion, is also marked for the three samples.

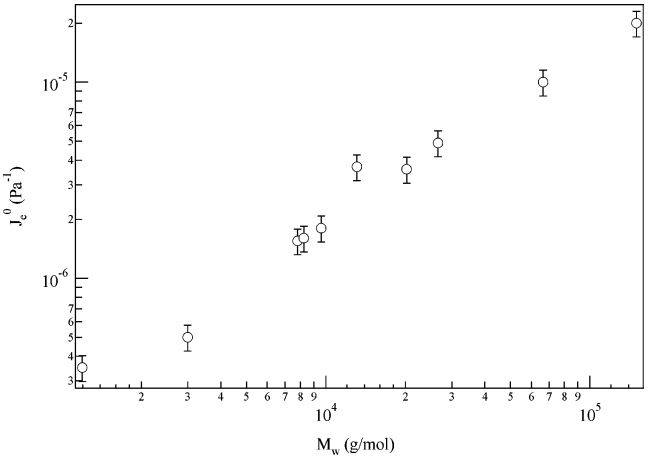

Figure 4. Measured J_e^0.

compliance J_e^0, which is defined[1] as follows:

$$J_e^0 = \lim_{\omega \to \infty} \frac{G'}{G''^2} \tag{6}$$

Figure 4 shows J_e^0 calculated at $T = T_r = 270$ K (open circles) as a function of the molar mass for all PEA samples.

4. Discussion

4.1. Mass-Dependent Thermal Behavior. As is known from the literature (for example, refs 2 and 25−27 and references therein) and is also easily checked from Tables 2 and 3, the parameters of VF and WLF laws present a molar mass dependence. Several empirical functional behaviors have been suggested to describe these changes with molar mass.

In the framework of the free volume approach, the VF (eq 3) and WLF (eq 4) parameters are related by

$$c_1 = \frac{B}{f_r \ln 10}, \quad c_2 = \frac{f_r}{\alpha} = T_r - T_0, \quad c_1 c_2 = \frac{B}{\alpha \ln 10} = \frac{T_b}{\ln 10} \tag{7}$$

where f_r is the free volume ratio at the reference temperature and B is a constant.[28]

The unique molar-mass-dependent quantity in the expression of T_b, or c_1c_2, is α, the latter being the thermal expansion coefficient of the free volume.[2] Expanding α at the first order on the inverse of molar mass as[27]

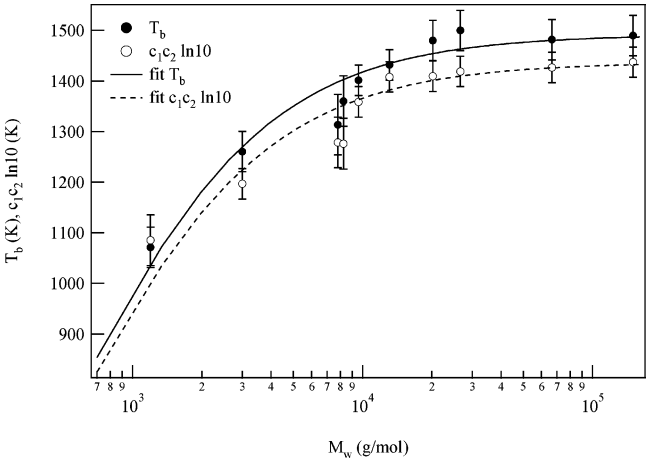

Figure 5. PEA's molar mass dependence of T_b (filled marks and solid line) and c_1c_2 ln 10 (empty marks and dashed line).

$$\alpha(M) = \alpha(\infty)(1 + M_{T_b}^{\infty}/M) \tag{8}$$

one finds that $T_b(M)$ is given by the relationship[25,26]

$$T_b(M) = T_b(\infty)\left(1 + \frac{M_{T_b}^{\infty}}{M}\right)^{-1} \tag{9}$$

so that $T_b(\infty)$ is $B/\alpha(\infty)$.

In Figure 5, the mass dependence of T_b and c_1c_2 ln 10 (Table 3) is compared with the relevant curves obtained according to eq 9. In both the cases the fitting parameter $M_{T_b}^{\infty}$ is found as $M_{T_b}^{\infty} = 520$ g/mol, while the asymptotic values $T_b(\infty)$ and c_1c_2-(∞) ln 10 are found to be different with values of 1490 and 1440 K, respectively, because in the derivation of eq 7 the quantity $b_{Tr}(T)$ was neglected. It is worth nothing that a value of $\alpha/B \approx 6.8 \times 10^{-4}$ K^{-1} is obtained in agreement with similar systems.[2]

Literature studies have suggested for the mass dependence of the Vogel temperature T_0:[26]

$$T_0(M) = T_0(\infty)\left(1 + \frac{M_{T_0}^{\infty}}{M}\right)^{-1} \tag{10}$$

Although from inspection of Figure 6 it is possible to conclude that eq 10 fits well the experimental data from PEA samples, because c_2, and thus T_0, scale as f_r/α, the mass dependence of these parameters cannot be taken in the proper account in eq 10. In fact, both the quantities α and f_r, the latter depending on T_r and on the chain-end effect on the free volume,[29] vary with molar mass. Therefore, the function $T_0(M)$ is not simply described by the approximation of eq 10, and both the α and the f_r mass dependence should be considered.

As a simple ansatz one could consider the growth of free volume with the tail concentration at low masses[29] and write a M expansion of $f_r(M)$ as $f_r(\infty)(1 + M_{c1}^{\infty}/M)$. The inset of Figure 6 supports this hypothesis, where $c_1 \propto 1/f_r$ and a law

$$c_1(M) = c_1(\infty)\left(1 + \frac{M_{c1}^{\infty}}{M}\right)^{-1} \tag{11}$$

are compared. It is apparent that experimental data agree with the theoretical curve. In the present case the fitting parameters

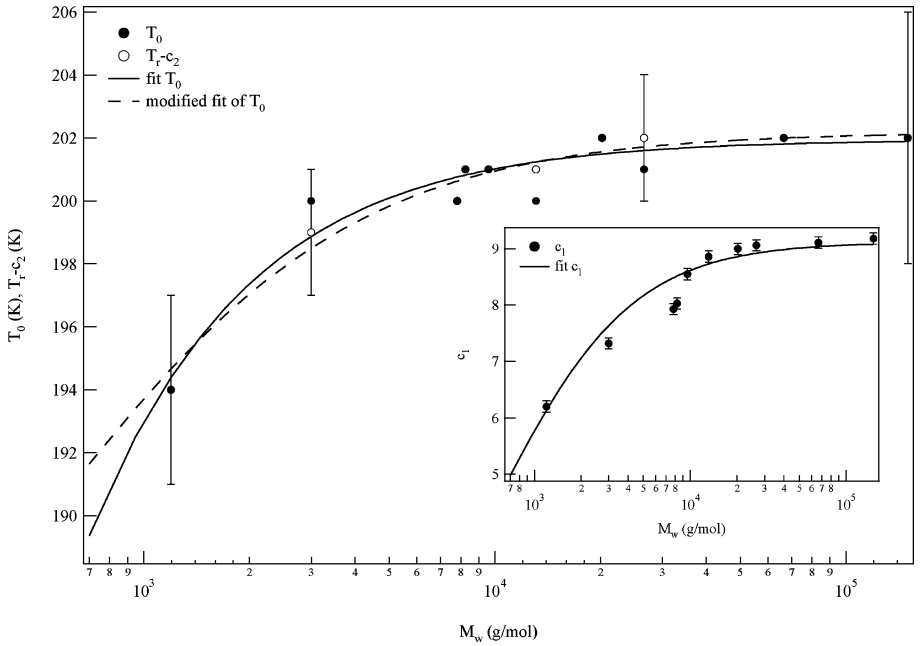

Figure 6. Molar mass dependence of T_0 and its fits according to both the literature (eq 10) and the modified equation (eq 12) here proposed. The inset shows the molar mass dependence of c_1.

resulted to be $c_1(\infty) = B/(\ln 10\ f_r(\infty)) = 9.12$ and $M_{c1}^{\infty} = 580$ g/mol. Adopting this mass dependence on f_r, one could therefore rewrite the function $T_0(M)$ (see eq 7 and related considerations) as

$$T_0(M) = \underbrace{\left(T_r - \frac{f_r(\infty)}{\alpha(\infty)}\right)}_{T_0(\infty)} \frac{M+W}{M+M_{T_b}^{\infty}}, \tag{12}$$

where

$$W = \frac{\dfrac{T_r}{T_b(\infty)} M_{T_b}^{\infty} - \dfrac{1}{c_1(\infty)\ln 10} M_{c1}^{\infty}}{\dfrac{T_r}{T_b(\infty)} - \dfrac{1}{c_1(\infty)\ln 10}} \tag{13}$$

The experimental fits of T_0 with eq 10 and with the proposed eq 12 are reported in Figure 6. By inspection, the two fits show almost the same behavior, except for the very low molar masses where the curves obtained from eq 10 underestimate T_0 with respect to eq 12.

In the mass range of our PEA samples, eq 10 and eq 12 both provide a good description of the data. However, in other systems,[30] literature studies have shown that eq 10 does not provide a proper description of T_0 for molar mass ranging from oligomers to high polymers. Moreover, the parameters of eq 10 cannot be connected to any microscopic quantity. In the present PEA case, fitting the experimental data with eq 10 provides the parameter $T_0(\infty) = 202$ K, as expected from Table 3, and $M_{T_0}^{\infty} = 46$ g/mol. On the other hand, from eq 12, the value of $M_{T_b}^{\infty}$ is 530 g/mol, which is consistent with the outcome for $M_{T_b}^{\infty}$ from eq 9. The value of the parameter W is 480 g/mol, while $T_0(\infty) = 202$ K.

A further test of the consistence of the suggested fitting laws (eqs 12 and 13) is given by substituting in eq 13 the parameter values obtained for $T_b(M)$ from eq 9 and for $c_1(M)$ from eq 11. One obtains the value of 490 g/mol as a prediction for W, nicely close to the value provided by directly fitting the data.

The Fox−Flory[31] empirical law

$$T_g(M) = T_g(\infty) - \frac{K}{M} \tag{14}$$

describes another important mass-dependent temperature of the polymer, the glass transition temperature T_g, in terms of tail free volume per unit volume. This can be expressed as $2\theta\rho N_A/M$, θ being the free volume of the chain tail, N_A the Avogadro number, and ρ the density. In fact, assuming the free volume ratio f at T_g to be independent of the molar mass, the exceeding free volume introduced by chain ends should be therefore compensated by the thermal contraction

$$2\theta\rho N_A/M = \alpha(T_g(\infty) - T_g(M)) \tag{15}$$

Equation 15 provides the expression

$$T_g(M) = T_g(\infty) - \frac{2\theta\rho N_A}{\alpha M} \tag{16}$$

Quite reasonably, the quantity θ can be considered independent of the polymer length because the tail mobility is not affected by how much chains are long. Comparing eq 14 and eq 16, K can be written as

$$K = \frac{2\theta\rho N_A}{\alpha} \tag{17}$$

The Fox−Flory law assumes K as a constant; however, in its formulation (eq 17) the mass dependence of the thermal expansion coefficient α could be explicited. As previously discussed, α scales as $\alpha_\infty(1 + M_{T_b}^{\infty}/M)$;[27] thus, a modified Fox−Flory law is easily obtained:

$$T_g(M) = T_g(\infty) - \underbrace{\frac{2\theta\rho N_A}{\alpha(\infty)}}_{K'} \frac{1}{M_{T_b}^{\infty} + M} \tag{18}$$

Note that the functional form of eq 18 derives quite naturally from the explicited α dependence on the mass, providing in such a way a direct meaning to the parameters which appear

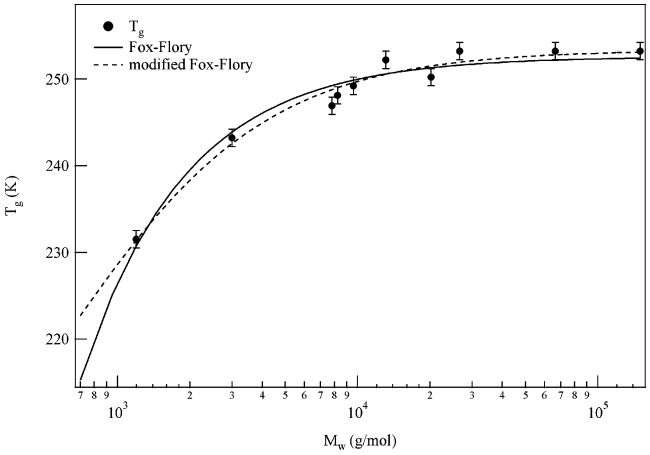

Figure 7. T_g dependence on the mass for PEAs. Fits of Fox−Flory law (solid line) and modified Fox−Flory (dashed line) are also reported.

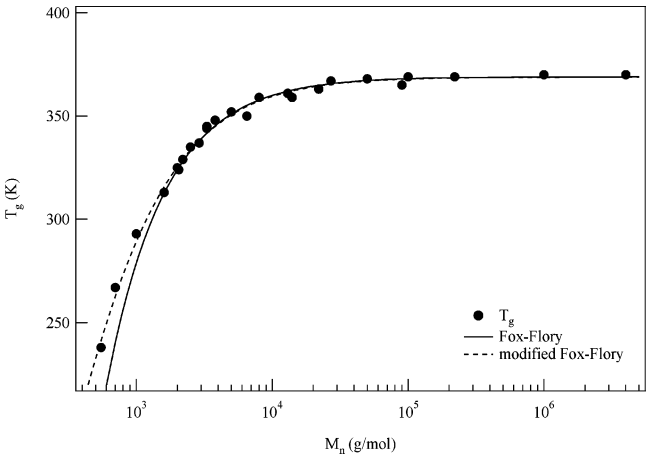

Figure 8. Data of T_g from ref 33 fitted with the Fox−Flory law and the modified Fox−Flory law proposed in this work. The latter better agrees with the experimental results.

determinated by the physical and structure properties of the series of homologue polymers.

From Figure 7, it is seen that, in the examined range of masses, both the curves obtained from eq 14 and eq 18 agree with the measured values of T_g of the series of PEAs, but the form of the original Fox−Flory law generates values lower than the modified eq 18 for very low molar masses. This behavior led Kanig and Uberreiter[32] to introduce the empirical dependence $T_g(M) = (1/T_g(\infty) + C/M)^{-1}$ to better describe the $T_g(M)$ behavior in the oligomers studied in their experiment. Another example is found for polystyrene samples. In Figure 8, a fit of these latter data[33] with the eq 18 here proposed appears more satisfactory than one with a Fox−Flory law.

A confirmation of the effectiveness of eq 18 in PEAs is given by the value of $M^{\infty}_{T_b}$ considered in the fit as a free parameter. It resulted to be 550 g/mol, in good agreement with the values previously obtained from the study of $T_0(M)$ and $T_b(M)$. The other two fitting parameters in eq 18, $T_g(\infty)$ and K', are evaluated respectively as 253 K and 38 000 K g/mol. The fitting procedure of the data with a Fox−Flory law (eq 14) gives $T_g(\infty) = 253$ K and, instead, $K = 26\,000$ K g/mol.

To gain more information, the interpretation in terms of free volume of the VF and WLF parameters of PEA polymers can be pursued by focusing our attention on the polymeric properties at the glass transition temperature T_g. It is known that some portion of free volume is necessary to achieve chain mobility at the glass transition temperature.[34] At T_g as the reference

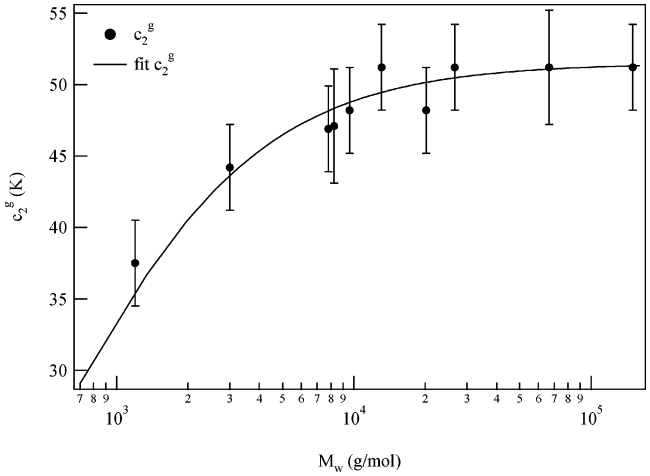

Figure 9. Dependence of c_2^g on the molar mass for PEAs. The continuous line refers to a fit according to the law $c_2^g(\infty)(1 + M^{\infty}_{T_b}/M)^{-1}$.

Table 4. WLF Parameters at T_g; PEAs Are Listed in Order of Increasing Molar Mass M_w

sample	c_1^g	c_2^g (K)	sample	c_1^g	c_2^g (K)
PEA15R	12.6 ± 1.1	37 ± 3	PEA02R	12.0 ± 0.8	51 ± 3
PEA16R	11.8 ± 1.0	44 ± 3	PEA04R	12.7 ± 0.8	48 ± 3
PEA17R	11.8 ± 0.8	47 ± 3	PEA05R	12.0 ± 0.8	51 ± 3
PEA01R	11.8 ± 1.2	47 ± 4	PEA06R	12.1 ± 1.2	51 ± 4
PEA18R	12.2 ± 0.8	48 ± 3	PEA20R	12.2 ± 0.8	51 ± 3

temperature, the fractional free volume f_g should be a constant; thus, according to eq 7, c_1^g is expected to be a constant, while c_2^g is expected to show only the molar mass dependence of $1/\alpha$.

These hypotheses can be validated by extrapolating c_1^g and c_2^g from the c_1 and c_2 values obtained from the experiments: c_1^g results to be about 12 (Table 4), while a fit of c_2^g according to the law $c_2^g(\infty)(1 + M^{\infty}_{T_b}/M)^{-1}$ gives as fitting parameters $c_2^g(\infty) = 51$ K and $M^{\infty}_{T_b} = 540$ g/mol (Figure 9), as already obtained dealing with the T_b, T_0, and T_g cases. An estimation of $f_g/B = 1/(c_1^g \ln 10)$ provides the value 0.036.

From all the above results, the ratio between the fractional chain-end free volume, $\bar{\theta} = \theta\rho N_A/(nM_0)$, and the fractional chain free volume at T_g, f_g, may be evaluated as

$$\frac{\bar{\theta}}{f_g} = \frac{K'}{2c_2^g(\infty)nM_0} = \frac{3.7}{n} \qquad (19)$$

nM_0 is the molar mass of the polymer tail, and M_0 is the polymeric repeating unit molar mass. The coefficient $c_2^g(\infty)$ is the $c_2(\infty)$ WLF coefficient, extrapolated at T_g by means of $c_2^g(\infty) = c_2(\infty) + T_g(\infty) - T_r$. If $n \simeq 4$, the two volumes would be equal, so T_g would be prevented from decreasing with polymeric mass; this would suggest that chain tails are not longer than $n = 3$ repeating units. This seems to be confirmed by literature simulations[11] where the tail free volume is evaluated as $\bar{\theta} \approx 2f_g$, as predicted by eq 19 in the case $n = 2$.

4.2. Mass Dependence of Material Parameters. The evaluation of other features of the polymeric mass dependence can be carried out by considering the behavior of the material parameters such as the zero-shear viscosity, the plateau modulus, and the steady-state compliance.

The shear viscosity η is expressed in terms of the shear modulus $G(t)$ as

$$\eta = \int_0^{\infty} G(t)\,dt \qquad (20)$$

The Rouse model provides for the shear modulus

$$G(t) = \frac{\rho RT}{M} \sum_p \exp\left(-\frac{2tp^2}{\tau_R}\right) \tag{21}$$

while according to the reptation scenario it should be

$$G(t) = G_N^0 \begin{cases} \left(\frac{\tau_e}{t}\right)^{\frac{1}{2}} & t < \tau_e; \\ \sum_{p:\text{odd}} \frac{8}{p^2\pi^2} \exp\left(-\frac{tp^2}{\tau_d}\right) & t > \tau_e. \end{cases} \tag{22}$$

where τ_R, τ_e, and τ_d are respectively the Rouse, the entanglement, and the disengagement times.[1] From the above relationships it is obtained:

$$\eta = \begin{cases} \frac{\rho RT}{M} \frac{\tau_R}{2} \sum_{p=1}^{\infty} p^{-2} = \frac{\pi^2}{12} \frac{\rho RT}{M} \tau_R \propto M & M < M_e \\ \frac{\pi^2}{12} G_N^0 \tau_d \propto M^3 & M > M_e, \end{cases} \tag{23}$$

where M_e is the entanglement mass.[1]

As a matter of fact, the experimental polymeric shear viscosity behavior deviates from eq 23: approximatively a kind of power dependence on the mass is observed up to a critical mass M_c (about 2.0−2.4 M_e), while above M_c, the mass dependence of the viscosity follows a power law with exponent 3.4. The power dependence at high molar masses can be explained by means of the contour length fluctuation theory,[1] even if recent theories point out that a more complex dependence should be expected and the 3.4 power law could be only due to an averaged slope in a certain range of molar masses.[35] The reason why the crossover happens at M_c instead of M_e is still an open issue.[36] The fact that below the critical mass M_c, the linear dependence is not observed[29] arises from the different contributions of the free volume of the chain tails.

A viscosity correction was therefore suggested in the literature[29] in order to avoid the differences in free volume introduced by the different concentration of polymer tails as the polymeric mass is varied. In fact, the accessible volume, greater to tails than to chains, provides greater mobility to shorter polymers, in which the chain-ends concentration is higher. A consequence of this fact is the lowering of the glass transition temperature T_g as the molar mass M is lowered, according to eq 14 and eq 18 of this and other works.[31] Therefore, an iso-free-volume correction is adopted to rescale the shear viscosity to the same friction coefficient value.[29,37]

This is accomplished by observing that the shear viscosity η can be written as

$$\eta = \zeta(T,M)\, F(M) \tag{24}$$

where ζ and F are an effective monomeric friction coefficient and a structural factor, respectively.[29] F depends only on the mass M, while $\zeta(T,M)$ is affected by the temperature and tail concentration, the latter being however negligible in very long chains. Thus, the identity $\zeta(T,M) = \zeta^\infty(T)$ can be set for high polymeric masses.

To evaluate only the F contribution to the η isothermal dependence on molar mass, η could be rescaled by the ratio $\zeta^\infty(T)/\zeta(T,M)$, which eliminates the tail free volume effects on the η mass dependence. This ratio can be evaluated as follows. First, one notes that in a series of homologue polymers ζ varies only with the free volume ratio f.[29] f depends on both the mass and temperature, and the same value of f corresponds at different couples of the (T, M) variables. Therefore, one writes

$$\frac{\zeta^\infty(T)}{\zeta(T,M)} = \frac{\zeta(f^\infty)}{\zeta(f)} \tag{25}$$

According to eq 24, one has

$$\frac{\zeta(f^\infty)}{\zeta(f)} \frac{F(M)}{F(M)} = \frac{\eta(f^\infty)}{\eta(f)} \tag{26}$$

At a fixed temperature, from the Doolittle equation[28] and eq 7, it follows

$$\frac{\zeta^\infty}{\zeta(M)} = 10^{c_1(\infty) - c_1(M)} \tag{27}$$

$c_1(\infty)$ is the c_1 value for the highest molar masses which tends to a constant value (Table 3 and Figure 6). Finally, the iso-free-volume corrected shear viscosity is obtained multiplying the ratio in eq 27 times the viscosity at the reference temperature T_r at which $c_1(M)$ and $c_1(\infty)$ were obtained from horizontal shift parameters via a WLF fit.

The iso-free-volume correction has been carried on the PEA series at the three reference temperatures T_r: 270, 291, and 305 K. From the three experimental sets of $a_{Tr}(T)$ data, the c_1 parameters are evaluated for all the different PEA samples (Table 5 for T_r = 291 and 305 K; Table 3 for 270 K). It is then possible to calculate the ratio ζ^∞/ζ according to eq 27 and operate the correction of η on the lowest masses.

Figure 10 shows the experimental and iso-free-volume corrected viscosity of PEA series at the reference temperatures. The two expected asymptotes $\eta \sim M$ at low masses and $\eta \sim M^{3.4}$ for the highest ones are also reported. As one can see, the crossover between the two power law regions is very sharp at M_c, where the two asymptotes intersect. This behavior is usually described by the relationship[29]

$$\eta(M_w) = AM_w\left[1 + \left(\frac{M_w}{M_c}\right)^\beta\right] \tag{28}$$

and the exponent of the mass dependence at high molar masses is given by $\beta_\infty = \beta + 1$. The solid curves in Figure 10 were calculated by using eq 28, and each of them provided the common value for the β_∞ parameter of 3.40 ± 0.04. On the other hand, the critical mass and the prefactor A are different for the different reference temperatures. It is found: at T_r = 270 K, M_c = 25 800 ± 500 g/mol and A = 145 ± 5 Pa s mol/g; at T_r = 291 K, M_c = 26 500 ± 500 g/mol and A = 1.02 ± 0.02 Pa s mol/g; at T_r = 305 K, M_c = 26 400 ± 500 g/mol and A = 0.083 ± 0.001 Pa s mol/g.

Table 5. WLF Coefficients for Iso-Free-Volume Corrections of Zero-Shear Viscosity at T_r of 291 and 305 K; Samples Are Listed in Order of Increasing Molar Mass M_w

	T_r = 291 K		T_r = 305 K	
sample	c_1[19]	c_2 (K)[19]	c_1[19]	c_2 (K)[19]
PEA15R	4.9	97	4.3	111
PEA16R	5.6	91	4.8	106
PEA17R	6.1	91	5.3	105
PEA01R	6.1	90	5.3	104
PEA18R	6.3	90	5.7	104
PEA02R	6.5	90	5.7	104
PEA04R	6.9	89	5.9	103
PEA05R	6.8	90	6.0	103
PEA06R	6.9	89	6.0	103
PEA20R	7.0	89	6.1	103

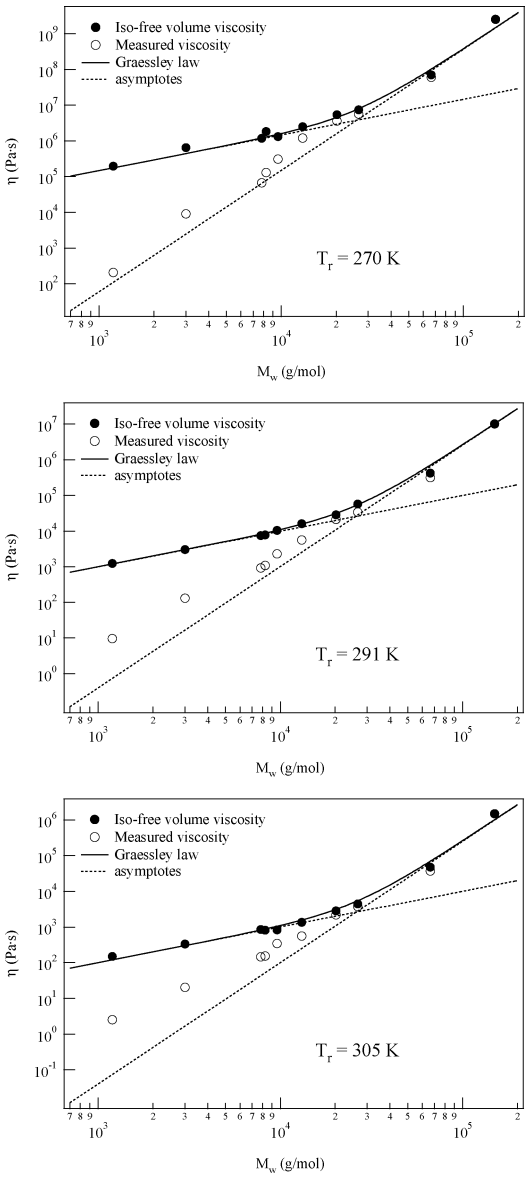

Figure 10. Viscosity dependence on the molar mass at three different reference temperatures. The measured viscosity (open circles) and the iso-free-volume-corrected viscosity $\eta(M_w)$ are shown. After the correction, η shows a linear behavior until the critical mass M_c is reached; for heavier masses, $\eta \propto M_w^{3.4}$.

From eq 23 it is possible to make explicit the expression of A of eq 28:

$$A = \frac{\pi^2}{12}\frac{\rho RT}{M^2}\tau_R = \frac{\rho N_a b^2 \zeta_0}{36 M_0^2} \tag{29}$$

where b is the length of one polymeric segment and ζ_0 the monomeric friction coefficient. It follows

$$b^2\zeta_0 = \frac{36 A M_0^2}{\rho N_a} \tag{30}$$

which gives $b^2\zeta_0(270\text{ K}) = (7.7 \pm 0.3) \times 10^{-23}$ N m s, $b^2\zeta_0(291\text{ K}) = (5.4 \pm 0.1) \times 10^{-25}$ N m s, and $b^2\zeta_0(305\text{ K}) = (4.4 \pm 0.1) \times 10^{-26}$ N m s. Assuming that $b \approx 6-7$ Å[38] and that, according also to eq 24, $\zeta_0(T)$ scales as[2]

$$\zeta_0(T) = \zeta_0^\infty \exp\left(\frac{T_b(\infty)}{T - T_0(\infty)}\right) \tag{31}$$

a VF fit of the data allows the evaluation of the free parameter ζ_0^∞. The inspection of Figure 11 shows that $\zeta_0(T)$ data follow the theoretical curve of eq 31 by setting the values $T_0(\infty) = 202$ K and $T_b(\infty) = 1490$ K. It is found $\zeta_0^\infty = (6.3 \pm 0.2) \times 10^{-14}$ N s/m.

It is known that the critical mass M_c is related to the entanglement mass M_e, being $M_c/M_e \approx 2.0-2.4$.[1] This finding may be checked also in our PEA samples. In fact, the entanglement mass M_e can be computed from the plateau modulus G_N^0 of the storage moduli G' master curves at the reference temperature as[20]

$$M_e \equiv \frac{\rho RT_r}{G_N^0} \tag{32}$$

From the G_N^0 values drawn from the master curves of PEA05R, PEA06R, and PEA20R shown in Figure 3, it is obtained $M_e = 12\,000$ g/mol at 270 K, $M_e = 12\,300$ g/mol at 291 K, and $M_e = 11\,800$ g/mol at 305 K, resulting in a constant ratio $M_c/M_e = 2.2 \pm 0.1$ in this temperature range.

In Figure 12, the scaled iso-free-volume corrected viscosities $\eta(M)/\eta(M_c)$ at the temperatures of 270, 291, and 305 K are plotted as a function of the mass and compared with the theoretical dependence predicted by the Rouse model and the McLeish model for linear entangled polymers.[35] As one can see, the data well agree with the theoretical curves. This comparison provides a consistency check for our data, but also an independent test of the theory[35] by using a different chemistry.

From the master curves, the steady-state shear compliance J_e^0 is calculated. At the frequencies of the terminal region, the polymeric chains have completely relaxed, and therefore the effects of molar mass and polydispersity can be detected. In monodisperse polymers, the empirical equation[34] has been proposed for the molar mass dependence of steady-state compliance

$$J_e^0 = \underbrace{\frac{2M_c'}{5\rho RT}}_{D}\left[1 - \exp\left(-\frac{M}{M_c'}\right)\right] \tag{33}$$

M_c' is a second critical mass, different from M_c. A plateau should be found for high molar masses, while the Rouse behavior $J_e^0 = 2M/(5\rho RT)$ is expected for low polymeric masses. In Figure 13 the J_e^0 data are shown.

Almost all PEA samples are nearly monodisperse; however, PEA15R, PEA06R, and PEA20R show polydispersity greater than 1.15; consequently, the J_e^0 data of these latter samples could not follow eq 33. Several attempts to correlate J_e^0 with mass distributions of polymers have been developed. The most accredited relationship is $J_e^0 \propto (M_z/M_w)^{3.7}$,[3,4] but exponents in the range of 2.5−4.0 have been also found.[39] In this work the trend of steady-state compliance could be compatible with a law $(M_z/M_w)^a$ with $a \approx 3.7$. Once J_e^0 data have been corrected according to this choice, the steady-state compliance of PEA samples can be rescaled to the common value of polydispersity $M_z/M_w = 1$.

A minimum square fit of iso-polydispersity-corrected values of J_e^0 with D and M_c' as free parameters in eq 33 is therefore carried out, and it is reported in Figure 13. The fit nicely follows the experimental data of the PEA's steady-state compliance and

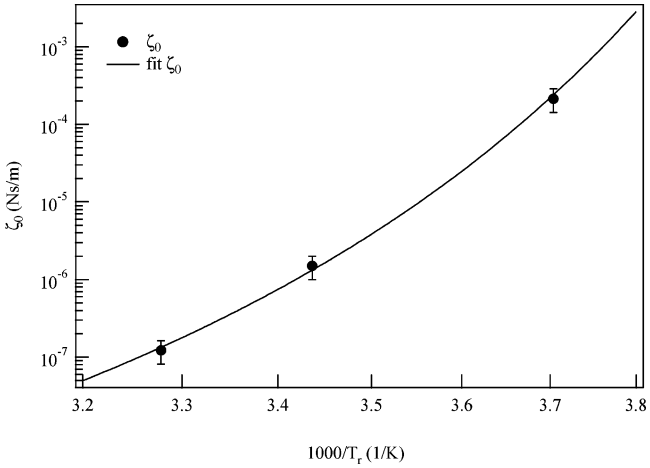

Figure 11. Temperature dependence of the monomeric friction coefficient ζ_0 as obtained from eq 30. The superimposed line is calculated according to eq 31 with $T_0(\infty)$ set at the value 202 K and $T_b(\infty) = 1490$ K.

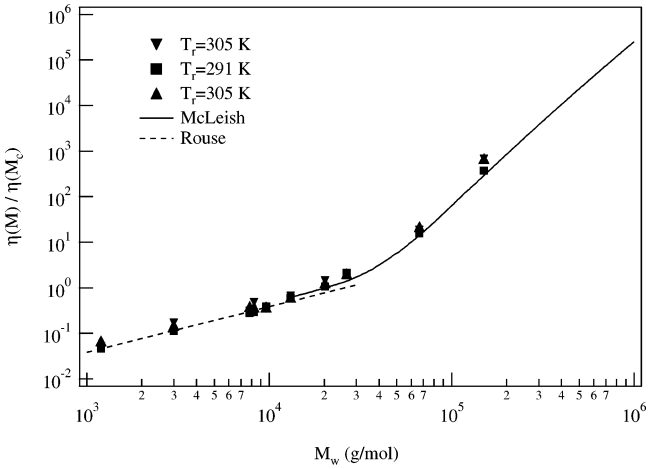

Figure 12. Rescaled iso-free-volume-corrected viscosities $\eta(M)/\eta(M_c)$ of PEAs at the temperatures of 270, 291, and 305 K. The mass dependences of viscosity according to the Rouse (dashed line) and the McLeish[35] (continuous line) models are also shown.

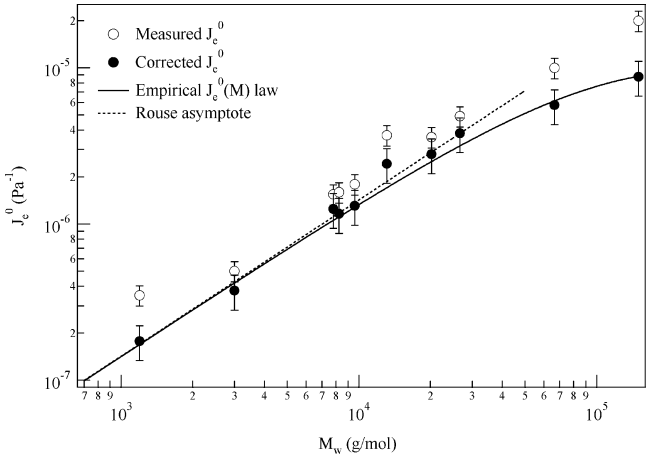

Figure 13. Measured J_e^0 (open circles) compared with the behavior of the empirical law of eq 33 (continuous line). Corrected data (filled circles) follow eq 33 with parameters $M_c' = 70\,000 \pm 9000$ g/mol and $\rho \approx 1.2 \pm 0.2$ g/cm^3. The Rouse prediction $J_e^0 \propto M_w$ (dashed line) for low molar masses is also reported.

for the parameters provides the values $D = (10 \pm 2) \times 10^{-6}$ Pa^{-1} and $M_c' = 70\,000 \pm 9000$ g/mol. Being $T_r = 270$ K, then the value of D allows one to evaluate ρ as 1.2 ± 0.2 g/cm^3. This value agrees with the value reported in the literature[17] and adopted in this work. It is also easy to verify the well-known[1] finding $M_c' \approx 3M_c \approx 6M_e$.

5. Summary

In the present paper, we have carried out a study of thermorheological properties of nearly monodisperse poly(ethyl acrylate) samples, synthesized according to a recent literature procedure. The experimental data of zero-shear viscosity and complex modulus were used to check the thermorheological simplicity of PEAs and to investigate the mass behavior of thermal parameters by resorting to the free volume approach.

The effects of the crossover between unentangled and entangled dynamics of the polymeric material was observed as a trend toward a plateau regime at high molar masses in the glass transition temperature and in the parameters of VF and WLF laws. Our observations are consistent with fitting laws suggested in the literature over the past years, but a comprehensive interpretation in terms of free volume is here proposed with a new coherent scenario for modified fitting laws, where the free parameters are connected to microscopic quantities. The consistency of this approach has been demonstrated. These fitting procedures allowed also the estimation of the length of the chain tails in agreement with literature simulations.

Moreover, from the study of the mass dependence of viscosity at different temperatures (with iso-free-volume corrections) and of the material functions plateau modulus G_N^0 and steady-state compliance J_e^0, the onset of entangled regime was estimated by the masses M_c, M_e, and M_c', which fulfilled the empirical rule $6M_e \approx 3M_c \approx M_c'$ as for conventional linear polymers. The estimation of the monomeric friction coefficient $\zeta_0(T)$ is also provided.

Acknowledgment. We acknowledge the Italian MIUR and INFM Pais project for financial support.

References and Notes

(1) Doi, M.; Edwards, S. F. *The Theory of Polymer Dynamics;* Oxford University Press: Oxford, 1986.
(2) Ferry, J. D. *Viscoelastic Properties of Polymers*, 3rd ed.; Wiley: New York, 1980.
(3) Mills, N. J. *Eur. Polym. J.* **1969**, *5*, 675.
(4) Mills, N. J.; Nevin, A. J. *J. Polym. Sci., Part A-2: Polym. Phys.* **1971**, *9*, 267.
(5) Lin, Y. H.; Juang, J. H. *Macromolecules* **1999**, *32*, 181.
(6) Vogel, H. *Z. Phys* **1921**, *22*, 645.
(7) Fulcher, G. S. *J. Am. Ceram. Soc.* **1925**, *8*, 339.
(8) Tamman, G.; Hesse, W. Z. *Anorg. Allg. Chem.* **1926**, *156*, 245.
(9) Andreozzi, L.; Faetti, M.; Giordano, M.; Palazzuoli, D.; Vittiglio, W.; Castelvetro, V.; De Vita, C. *Macromol. Chem. Phys.* **2002**, *203*, 1445.
(10) Xia, J.; Matyjaszewski, K. *Macromolecules* **1997**, *30*, 7697.
(11) McCormick, J. A.; Hall, C. K.; Khan, S. A. *J. Chem. Phys.* **2002**, *117*, 944.
(12) Sperling, L. H. *Introduction to Physical Polymer Science*, 3rd ed.; John Wiley & Sons: New York, 1996.
(13) Time of polymerization.
(14) SEC analyses with a light scattering detector provided $M_n = 22\,200$ g/mol and $M_w/M_n = 1.07$.
(15) The polymerization was carried out in anisole (4.6 mol/L) at 60 °C.
(16) The polymerization was performed in solution of anisole (5.7 mol/L) at 90 °C.
(17) Wen, J. In *Polymer Data Handbook*, Mark, J., Ed.; Oxford University Press: Oxford, 1999.
(18) Honerkamp, J.; Weese, J. *Rheol. Acta* **1993**, *32*, 57.
(19) The error on c_1 amounts to ± 0.1 and on c_2 to ± 2 K.
(20) Larson, R. G.; Sridhar, T.; Leal, L. G.; McKinlkey, G. H.; Likhtman, A. E.; McLeish, T. C. B. *J. Rheol.* **2003**, *47*, 809.
(21) Graessley, W. W. *J. Polym. Sci., Polym. Phys. Ed.* **1980**, *18*, 27.
(22) Fetters, L. J.; Lohse, D. J.; Milner, S. T.; Graessley, W. W. *Macromolecules* **1999**, *32*, 6847−6851.
(23) Wu, S. *J. Polym. Sci., Part B: Polym. Phys.* **1989**, *27*, 723.
(24) Lomellini, P.; Lavagnini, L. *Rheol. Acta* **1992**, *31*, 175.

(25) Richter, D.; Willner, R.; Zirkel, A.; Farago, B.; Fetters, L. J.; Huang, J. S. *Macromolecules* **1994**, *27*, 7437.
(26) Pearson, D. S.; Fetters, L. J.; Graessley, W.; Ver Strate, G.; von Meerwall, E. *Macromolecules* **1994**, *27*, 711.
(27) Pearson, D. S.; Ver Strate, G.; von Meerwall, E.; Schilling, F. C. *Macromolecules* **1987**, *20*, 1133.
(28) Doolittle, A. K. *J. Appl. Phys.* **1951**, *22*, 1471.
(29) Colby, R. H.; Fetters, L. H.; Graessley, W. W. *Macromolecules* **1987**, *20*, 2226.
(30) Capaccioli, S.; Casalini, R.; Lucchesi, M.; Lovicu, G.; Prevosto, D.; Pisignano, D.; Romano, G.; Rolla, P. A. *J. Non-Cryst. Solids* **2002**, *307*, 238.
(31) Fox, T. G.; Flory, P. J. *J. Appl. Phys.* **1950**, *21*, 581.
(32) Kanig, G.; Uberreiter, K. *J. Colloid. Sci.* **1952**, *7*, 569.
(33) Sokolov, A. "Physical properties of polymers: glass transition", Fall, 2004 web address: http://gozips.uakron.edu/ alexei/Lect37p2.pdf.
(34) Fuchs, K.; Friedrich, C.; Weese, J. *Macromolecules* **1996**, *29*, 5893.
(35) Likhtman, A. E.; McLeish, T. C. B. *Macromolecules* **2002**, *35*, 6332.
(36) For example, atomistic molecular dynamics simulations have shown that the Rouse model is still applicable to predict ζ up to M_c: Harmandaris, V. A.; Mavrantzas, D. N.; Theodorou, D. N.; Kröger, M.; Ram×c6rez, J.; Öttinger, H. C.; Vlassopoulos, D. *Macromolecules* **2003**, *36*, 1376.
(37) A straightforward isofriction correction can be also accomplished by rescaling viscoelastic quantities dependent on ζ with the segmental time. See for example: Pakula, T.; Vlassopoulos, D.; Fytas, G.; Roovers, J. *Macromolecules* **1998**, *31*, 8931. Islam, M. T.; Juliani; Archer, L. A.; Varshney, S. K. *Macromolecules* **2001**, *34*, 6438.
(38) Kholodenko, A. L.; Vilgis, T. A. *Phys. Rep.* **1998**, *298*, 251.
(39) Agarwal, P. K. *Macromolecules* **1979**, *9*, 342.

MA052190+